Optical constants of DUV/UV fluoride thin films

Chunrong Xue (薛春荣)[1,2,3*], Kui Yi (易 葵)[1], Chaoyang Wei (魏朝阳)[1], Jianda Shao (邵建达)[1], and Zhengxiu Fan (范正修)[1]

[1] *Shanghai Institute of Optics and Fine Mechanics, Chinese Academy of Sciences, Shanghai 201800, China*

[2] *Jiangsu Laboratory of Advanced Functional Materials, Changshu Institute of Technology, Changshu 215500, China*

[3] *National Synchrotron Radiation Laboratory, University of Science and Technology of China, Hefei 230029, China*

**E-mail: 99xcr@163.com*

Received August 8, 2008

High-refractive-index materials LaF_3, NdF_3, and GdF_3 and low-refractive-index materials MgF_2, AlF_3, and Na_3AlF_6 single thin films are deposited by a resistive-heating boat at different depositing rates and specific substrate temperatures on single crystal MgF_2 substrates. Transmittances of all fluoride thin films are measured using commercial spectrometer in the ambient atmosphere and under vacuum using synchrotron radiation instrument in the wavelength region from 190 to 500 nm. The optical constants of these materials are determined by envelope method and iterative algorithm on the basis of transmittance measurements.

OCIS codes: 310.6188, 310.6860, 160.4670.

doi: 10.3788/COL20090705.0449.

The optical constants of materials in the deep ultraviolet (DUV) spectral region are of interest to several areas of technology. Much research and investigation of oxide and fluoride materials for DUV and ultraviolet (UV) coatings[1−10] have been done, but only a few fluoride materials can be used due to their insufficient energy band gap[11−14].

We report the determination of optical constants of LaF_3, NdF_3, GdF_3, MgF_2, AlF_3, and Na_3AlF_6 thin films over the $190-500$ nm spectral range. It is found that LaF_3, NdF_3, and GdF_3 may be used as high-refractive-index film materials for constructing a high/low index pair with MgF_2, AlF_3, and Na_3AlF_6 being the useful low-index materials in the DUV/UV range.

We use the envelope method, which makes use of two envelope functions $T_{\lambda/2}$ and $T_{\lambda/4}$, to obtain the refractive indices. The positions of the extrema of $T_{\lambda/2}$ and $T_{\lambda/4}$ permit the extraction of a film thickness value that is used to complete the optical-constant extraction. Figure 1 shows the sketch of the envelope.

With a transmission measurement only, the complex refractive index as well as the thickness can therefore be derived. The transmittance T, the thickness d, the optical constants n and k can be given by[15]

$$T = \frac{AX}{B - CX + DX^2}, \quad (1)$$

$$n = [Q + (Q^2 - n_s^2)^{1/2}]^{1/2}, \quad (2)$$

$$k = -\frac{\lambda}{4\pi d}\ln X, \quad (3)$$

$$d \approx \frac{\lambda_m \cdot \lambda_{m+1}}{2(n(\lambda_m)\cdot\lambda_{m+1} - n(\lambda_{m+1})\cdot\lambda_m)}, \quad (4)$$

where

$$\begin{aligned}
A =& \; 16n_s(n^2+k^2),\\
B =& \; [(n^2+1)^2+k^2][(n+1)(n+n_s^2)+k^2],\\
C =& \; 2[(n^2-1+k^2)(n^2-n_s^2+k^2)\\
& -2k^2(n_s^2+1)]\cos 2\alpha - 2k[2(n^2-n_s^2+k^2)\\
& +(n_s^2+1)(n^2-1+k^2)]\sin 2\alpha,\\
D =& \; [(n-1)^2+k^2][(n-1)(n-n_s^2)+k^2],\\
Q =& \; 2n_s\cdot\frac{T_{\mathrm{top}}-T_{\mathrm{bottom}}}{T_{\mathrm{top}}\cdot T_{\mathrm{bottom}}}+\frac{n_s^2+1}{2},\\
X =& \; \frac{F-\sqrt{F^2-(n^2-1)^3\cdot(n^2-n_s^2)}}{(n-1)^3\cdot(n-n_s^2)},\\
F =& \; \frac{8n^2n_s}{T_i},\\
T_i =& \; \frac{2T_{\mathrm{top}}\cdot T_{\mathrm{bottom}}}{T_{\mathrm{top}}+T_{\mathrm{bottom}}},
\end{aligned}$$

n_s is the substrate refractive index, T_{top} and T_{bottom} are the upper and lower extreme points,

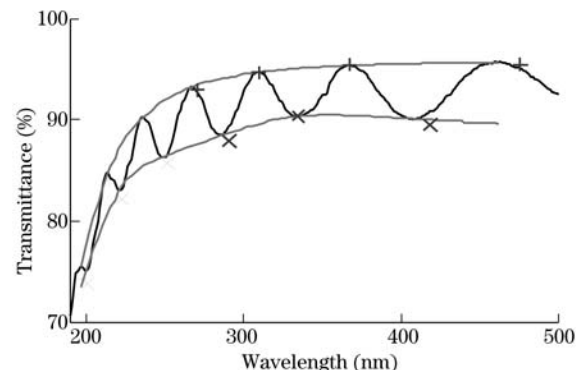

Fig. 1. Sketch of envelop curves.

 © 2009 Chinese Optics Letters

respectively, λ_m and λ_{m+1} are the adjacent maximum or minimum wavelengths.

The drawback of this method is that the indices derived from the envelopes are sensitive to the errors that occur in these functions, and there are great difficulties in high-absorption regions. To avoid this obstacle and to make it possible to take full advantage of the envelope method, we propose an approach in which linear interpolation (extrapolation) is used to build the envelopes over the whole spectral range. The details of this approach are as follows.

Step 1: with the transmission curve measured, sketch the upper and the lower envelopes.

Step 2: read the tangent points of the transmission curve with its envelopes over the whole spectrum. Calculate the refractive index by using Eq. (2).

Step 3: determine the interference order. The tangent points fulfill the envelope condition such as $2\alpha = m\pi$ where m is an integer. Ignoring the extinction coefficient, the quarter-wave condition is obtained as

$$nd = m\frac{\lambda}{4}. \quad (5)$$

The order at a reference point, for instance λ_3, can be estimated with the help of an adjacent maximum or minimum at λ_1. The order m_3 at λ_3 can be written as $m_3 = \frac{2}{(n_1\lambda_3)/(n_3\lambda_1)-1}$, where $\lambda_3 > \lambda_1$.

Generally, a pair of maxima or minima in the transparent region is chosen for the order estimation, because accurate envelopes can be obtained in that region. The estimated order might not be an integer, so that a close integer that is an even or an odd number, depending on whether the transmittance is maximum or minimum, will be assigned to that reference point. Once the order of the reference point is determined, the orders of the other data points can be inferred automatically.

Step 4: calculate the thickness by Eq. (5). At this stage, the thickness calculated by Eq. (5) will be dispersive when different data points are used for calculation. The dispersion might come from two aspects. Firstly, wrong orders are assigned to the data points. The effect of wrong orders can be seen as the thickness dispersion in the transparent region. A new set of orders close to the one from step 3 can then be re-selected for thickness calculations. This process can be repeated until the best set is found. The optimized order should yield the least thickness dispersion, especially in the transparent region. Secondly, dispersion may result from the erroneous refractive indices. To resolve this inherent error, we launch a two-stage iteration in which the influence of the envelopes is reduced to a minimum. Because the thickness d, the refractive index n, and the extinction coefficient k are connected to each other, these three parameters are then put into a merit function and optimized together in terms of a minimum searching process.

Step 5: iterate the optical constants. The average value of thickness from step 4 is used as the initial value for iteration. With the given thickness and the orders from step 3, more consistent n can be obtained by Eq. (5) for each data point. Once the index is determined, k can be calculated with Eq. (3).

Step 6: optimize the thickness. A merit function defined as $\Delta = \sum_i |T_i - T_{\mathrm{m}i}|$ is used to optimize the thickness. In the merit function, T_i is the transmittance calculated by the insertion of the thickness and optical constants into Eq. (1). $T_{\mathrm{m}i}$ is the corresponding measured transmittance. The goal of the optimization is to find a thickness value for which the merit function has a minimum value. A minimum bracketing method is used to search this thickness. For a new trial thickness, a new set of optical constants can be found through step 5.

Finally, the optimized optical constants at all points are fitted using the least-square fitting by Cauchy dispersion equation, $n(\lambda) = A_1 + \frac{A_2}{\lambda^2} + \frac{A_3}{\lambda^4}$, and the index dispersion formula $k(\lambda) = A_4 + A_5 \exp\left(\frac{\lambda}{A_6}\right)$. Then the dispersion curve of optical constants can be determined in the measured spectral band.

It has been shown that the optical loss of fluoride films is less when they are deposited by thermal evaporation rather than other deposition methods, including magnetron sputtering, ion beam assisted deposition, or ion beam sputtering[3−9]. In this work, all fluoride thin film coatings were deposited by thermal evaporation on 15-mm-diameter by 3-mm-thick magnesium fluoride substrate. The chamber was pumped out to a base pressure at less than 1.33×10^{-3} Pa before the evaporation process. The temperature of the MgF_2 substrate during deposition of the fluoride films was 270 °C. The pressure before and during deposition, P_0 and P, the deposition rates D_{R}, and the physical thicknesses of the films d are listed in Table 1.

The transmittances of the thin films were measured under vacuum through synchrotron radiation with a special vacuum UV measurement component in the National Synchrotron Radiation Laboratory (NSRL), the University of Science and Technology of China in Hefei and with a commercial spectrometer λ900 in the ambient atmosphere for 190 − 500 nm, respectively. Transmittance measurement results of LaF_3, NdF_3, GdF_3, MgF_2, AlF_3, and Na_3AlF_6 films deposited on MgF_2 substrates are given in Figs. 2 and 3.

Based on the measured transmittances, we can determine the optical constants according to the method introduced above. The corresponding optical constants are given in Figs. 4 and 5.

For high-index materials, the refractive index n is higher than 1.5 throughout the DUV/UV region. The extinction coefficient k has values of the order of 10^{-2} or lower throughout the DUV/UV region. Low-index material films indicate low values of refractive index n and a relatively small extinction coefficient k for wavelengths longer than 120 nm. It is found that LaF_3, NdF_3, and GdF_3 may be used as high-refractive index film materials

Table 1. Deposition Conditions

Material	P_0 ($\times10^{-3}$ Pa)	P ($\times10^{-3}$ Pa)	D_R (nm/s)	d (nm)
LaF_3	0.933	1.07	0.23	680
NdF_3	1.13	1.6	0.16	597
GdF_3	1.33	2.4	0.43	1007
MgF_2	1.33	1.47	0.21	664
AlF_3	1.2	1.47	0.6	947
Na_3AlF_6	1.2	1.33	0.42	1241

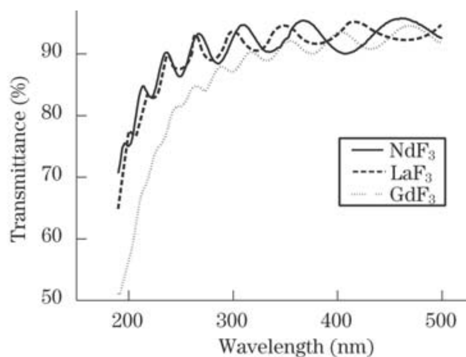

Fig. 2. Transmittances of LaF_3, NdF_3, and GdF_3 single layer films.

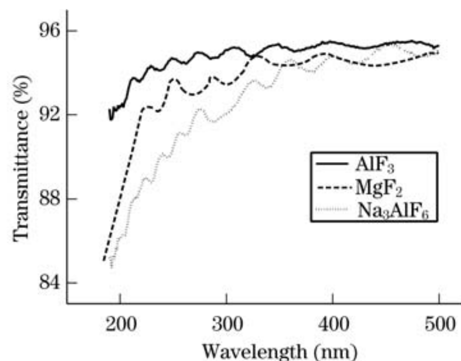

Fig. 3. Transmittances of MgF_2, AlF_3, and Na_3AlF_6 single layer films.

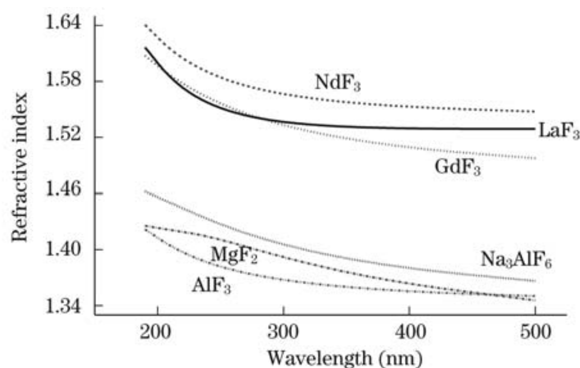

Fig. 4. Refractive indices of LaF_3, NdF_3, GdF_3, MgF_2, AlF_3, and Na_3AlF_6 single layer films.

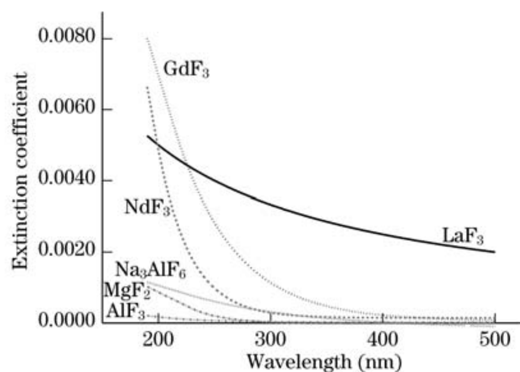

Fig. 5. Extinction coefficients of LaF_3, NdF_3, GdF_3, MgF_2, AlF_3, and Na_3AlF_6 single layer films.

for constructing a high/low index pair with MgF_2, AlF_3, and Na_3AlF_6 being the most useful low-index materials in the DUV band.

In conclusion, the determination of optical constants of LaF_3, NdF_3, GdF_3, MgF_2, AlF_3, and Na_3AlF_6 single layer coatings in the wavelength range from 190 to 500 nm has been presented. The envelope method provides a good initial step to start the iteration. The initial thickness provided by the envelope method is then modified by the iteration algorithm, which reduces the effect of the envelopes to a minimum. Iterative mathematical modeling of transmittance measurements provides a reliable way for determining the optical constants of thin films deposited on the weakly absorbing substrates. High values of refractive index make LaF_3, NdF_3, and GdF_3 useful materials for the DUV band, particularly for constructing a high/low index pair with MgF_2, AlF_3, and Na_3AlF_6 being the most useful low-index materials.

The authors would like to acknowledge Mr. G. Zhang for transmittance measurements and helpful discussions. This paper was supported by the National Natural Science Foundation of China under Grant No. 60678004.

References

1. H. Yu, Y. Cui, Y. Sheng, H. Qi, J. Shao, and Z. Fan, Chinese J. Lasers (in Chinese) **34,** 1557 (2007).
2. J. Yuan, H. Qi, Y. Zhao, Z. Fan, and J. Shao, Chin. Opt. Lett. **6,** 222 (2008).
3. S. Niisaka, T. Saito, J. Saito, A. Tanaka, A. Matsumoto, M. Otani, R. Biro, C. Ouchi, M. Hasegawa, Y. Suzuki, and K. Sone, Appl. Opt. **41,** 3242 (2002).
4. St. Günster, D. Ristau, A. Gatto, N. Kaiser, M. Trovò, M. B. Danailov, and F. Sarto, in *Proceedings of the 2004 FEL Conference* 233 (2004).
5. A. Gatto, R. Thielsch, J. Heber, N. Kaiser, D. Ristau, S. Günster, J. Kohlhaas, M. Marsi, M. Trovò, R. Walker, D. Garzella, M. E. Couprie, P. Torchio, M. Alvisi, and C. Amra, Appl. Opt. **41,** 3236 (2002).
6. A. Gatto, M. Yang, N. Kaiser, J. Heber, J. U. Schmidt, T. Sandner, H. Schenk, and H. Lakner, Appl. Opt. **45,** 1602 (2006).
7. E. T. Hutcheston, G. Hass, and J. T. Cox, Appl. Opt. **11,** 2245 (1972).
8. G. Hass, J. Opt. Soc. Am. **72,** 27 (1982).
9. R. Biro, K. Sone, S. Niisaka, M. Otani, Y. Suzuki, C. Ouchi, T. Saito, M. Hasegawa, J. Saito, A. Tanaka, and A. Matsumoto, Proc. SPIE **4691,** 1625 (2002).
10. W. R. Hunter, J. F. Osantowski, and G. Hass, Appl. Opt. **10,** 540 (1971).
11. St. Günster, H. Blaschke, D. Ristau, M. Danailov, M. Trovó, A. Gatto, N. Kaiser, F. Sarto, D. Flori, and F. Menchini, Proc. SPIE **5250,** 146 (2004).
12. A. Gatto, M. Yang, N. Kaiser, S. Günster, D. Ristau, M. Trovo, and M. Danailov, Appl. Opt. **45,** 7316 (2006).
13. F. Sarto, E. Nichelatti, D. Flori, M. Vadrucci, A. Santoni, S. Pietrantoni, S. Guenster, D. Ristau, A. Gatto, M. Trovò, M. Danailov, and B. Diviacco, Thin Solid Films **515,** 3858 (2007).
14. St. Günster, H. Blaschke, D. Ristau, A. Gatto, J. Heber, N. Kaiser, B. Diviacco, M. Marsi, M. Trovò, F. Sarto, S. Scaglione, and E. Masetti, Proc. SPIE **4932,** 422 (2003).
15. S.-C. Chiao, B. G. Bovard, and H. A. Macleod, Appl. Opt. **34,** 7355 (1995).